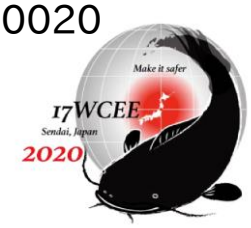



# Hysteretic model estimation of Y-type perfobond rib shear connectors

S.-H. Kim[1], D.Y. Kim[2], O. Han[3], S. Yoon[4]

[1] *Professor, School of Civil and Environmental Engineering, Yonsei University, Seoul 03722, Korea, sanghyo@yonsei.ac.kr*
[2] *Researcher, School of Civil and Environmental Engineering, Yonsei University, Seoul 03722, Korea, daeyoon@yonsei.ac.kr*
[3] *Researcher, School of Civil and Environmental Engineering, Yonsei University, Seoul 03722, Korea, oneilhan86@gmail.com*
[4] *Researcher, School of Civil and Environmental Engineering, Yonsei University, Seoul 03722, Korea, dbstnfh112@nacer.com*

## *Abstract*

This study analyzes the shear and hysteresis behavior of stubby Y-type perfobond rib shear connector and suggests its hysteretic model. To evaluate energy dissipation of stubby Y-type perfobond rib shear connectors, the different number of ribs (4 ribs, 6 ribs, and 8 ribs) are considered. Since the size of large number of ribs makes it difficult to proceed with an experiment, experiment on shear connectors which has small number of ribs are conducted.

The hysteretic study on stubby Y-type perfobond shear connector is performed with the adoption of the Bouc-Wen-Baber-Noori (BWBN) model, which can predict more accurate results and characterize the pinching behavior. Finally, the BWBN model parameters are predicted for stubby Y-type perfobond shear connectors with large number of ribs based on the experimental data of shear connectors with small number of ribs. To increase the accuracy of the energy dissipation prediction, small (1-4mm) and large (over 4mm) slip amplitudes are considered.

The main goal of this research is that the estimation on hysteretic behavior for large number of ribs from the hysteretic behavior of small number of ribs. Additionally, the other goal is to check the applicability of the BWBN model on different cyclic loading condition.

Keywords: Composite structure; Y-type perfobond rib shear connector; hysteresis behavior; cyclic loading; BWBN

## 1. Introduction

### 1.1 Y-type perfobond rib shear connector

In construction field, the stud type shear connector [1] and flat type shear connector [2] are widely used. Due to the workability of headed-stud-type connector, it is popular in construction field. However, it has weaknesses in the way that fatigue at connector roots and weakness under large slips cause failure [3,4]. Perfobond rib shear connector is another alternative of rigid shear connector, consisting of a flat steel plate with dowel holes. It provides prominent shear resistance of end bearing effect, dowel resistance and the resistance of transverse rebar placed through dowel holes [3,5-9]. Although it has a preeminent performance on shear resistance, it also has weakness on brittle fracture [3,5,10]. Recently, the Y-type perfobond rib shear connector with excellent shear strength and ductility was developed by Kim et al. [11]. This shear connector was initially designed for highway composite bridges. Kim et al. suggested the shear resistance equation for Y-type perfobond rib shear connector with various design variables, including the Y-rib dimensions, number of ribs, and concrete compressive strength [12,13]. Also, the effects of double-row Y-type perfobond rib shear connectors through push-out test was evaluated [14]. Later, conventional Y-type perfobond rib shear

connector was modified to use it in general buildings. Kim et al. evaluated hysteretic performance of stubby Y-type perfobond rib and compared the structural performance with stud shear connectors [15,16].

### 1.1 Test specimen

As shown in Fig. 1, stubby Y-rib has thickness of 8 mm, the height of 50 mm and the dowel diameter of 30 mm. The compressive strength of the concrete is 35 MPa and the concrete cylinder test is measured to 33.4 MPa on average. Steel is designed according to the Korea Highway Bridge Specifications [17] as shown in Table 1. Also, Styrofoam is attached on the bottom end of Y-ribs in to eliminate the end-bearing effect. There are two groups of specimens. One group consists of six specimens (Y4ribs-M, Y6ribs-M) for monotonic loading tests and nine specimens (Y4ribs-C, Y6ribs-C and Y-8ribs-C) for cyclic loading tests. The other group is the same with the first group.

Table 1 – Structural steel properties

| Type | Yield Strength (MPa) | Ultimate Strength (MPa) | Elongation (%) | Young's modulus (MPa) | Part |
|---|---|---|---|---|---|
| SS400 | 389 | 451 | 25.0 | 210,000 | Y-rib |
| SM490 | 452 | 560 | 19.0 | 210,000 | H-beam |
| SD400 | 400 | 639 | 17.3 | 210,000 | Rebar (D13) |

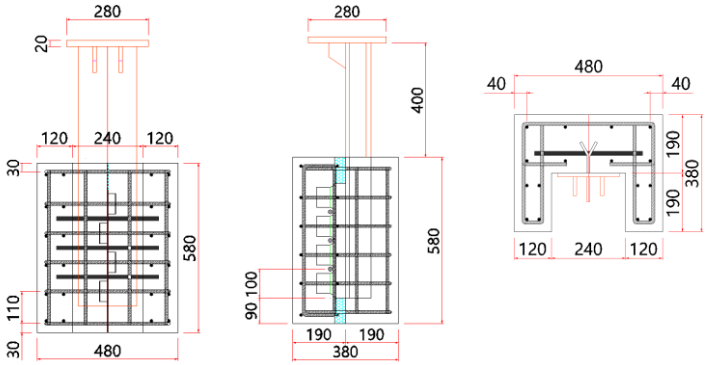


a) Dimensions of Y-4ribs specimen

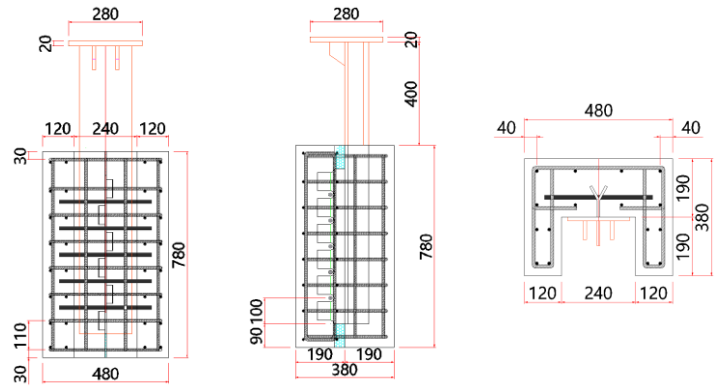


b) Dimensions of Y-6ribs specimen



 

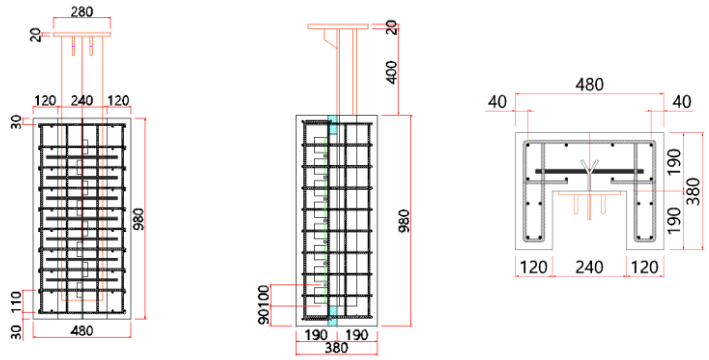


c) Dimensions of Y-8ribs specimen

Fig. 1 – Dimensions of Y-type perfobond rib shear connector (mm)

### 1.2 Test procedure

Experiment set-up of the Y-type shear connector is shown in Fig. 2. All the tests are conducted by a 1,000 kN universal testing machine (UTM). There are two different cyclic loading conditions for each group of specimens. Cyclic loading conditions for the Y-type shear connector consist of initial cyclic loading and cyclic loading. The first cyclic loading condition are indicated in Table 2. Test has been conducted until 16 mm slip, but BWBN hysteresis model is suggested until 8 mm slip since 16 mm slip is considered very large. The other cyclic loading condition is shown in Table 3 which which has different loading condition after 8mm slip.

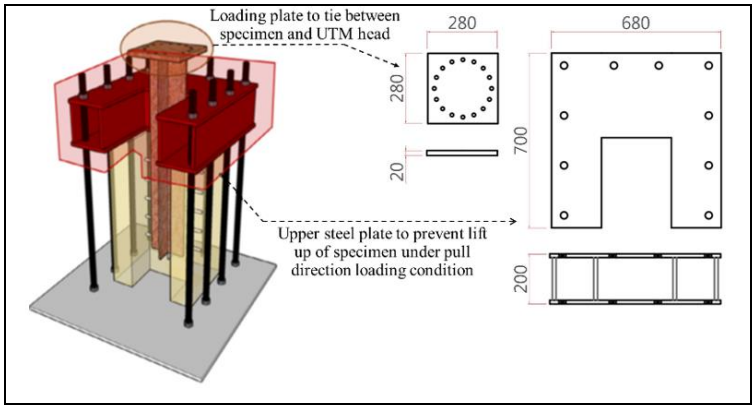


Fig. 2 – Experiment set-up

Table 2 –1st cyclic loading condition [18]

| Cycle No. | Slip (mm) | Note | Cycle No. | Slip (mm) | Note |
|---|---|---|---|---|---|
| 1 | ±0.02 | Initial loading | 10 | ±1 | Cyclic loading |
| 2 | ±0.03 | | 11 | ±2 | |
| 3 | ±0.04 | | 12 | ±3 | |
| 4 | ±0.06 | | 13 | ±4 | |
| 5 | ±0.09 | | 14 | ±8 | |
| 6 | ±0.12 | | 15 | ±8 | |
| 7 | ±0.18 | | 16 | ±8 | |
| 8 | ±0.27 | | | | |
| 9 | ±0.4 | | | | |



 

Table 3 – 2nd cyclic loading condition

| Cycle No. | Slip (mm) | Note | Cycle No. | | Slip (mm) | Note |
|---|---|---|---|---|---|---|
| 1 | ±0.02 | Initial loading | 10 | | ±1 | Cyclic loading |
| 2 | ±0.03 | | 11 | | ±2 | |
| 3 | ±0.04 | | 12 | | ±3 | |
| 4 | ±0.06 | | 13 | | ±4 | |
| 5 | ±0.09 | | 14 | | ±8 | |
| 6 | ±0.12 | | 15 | | ±8 | |
| 7 | ±0.18 | | 16 | | ±8 | |
| 8 | ±0.27 | | 17 | | ±4 | |
| 9 | ±0.4 | | 18 | | ±3 | |
| | | | 19 | | ±4 | |
| | | | 20 | | ±8 | |
| | | | 21 | | ±8 | |
| | | | 22 | | ±8 | |

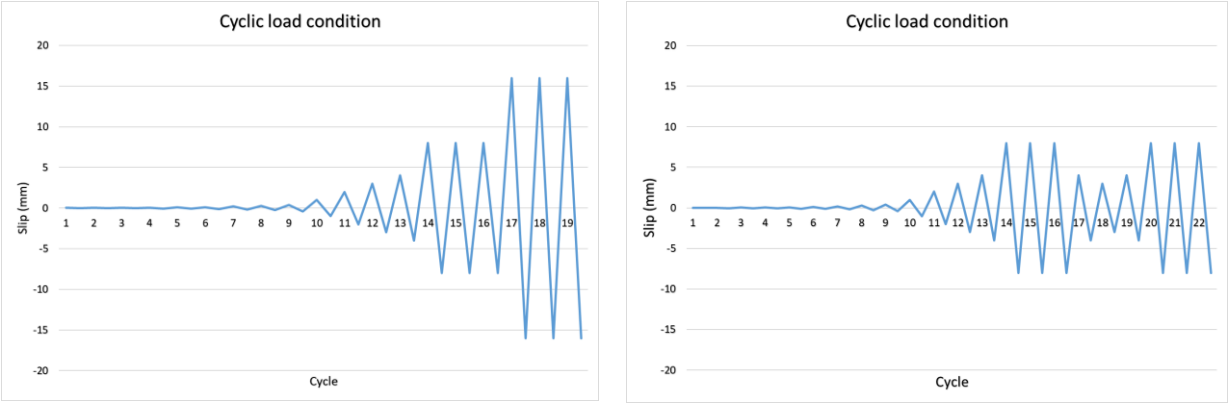


a) 1st cyclic loading condition b) 2nd cyclic loading condition

Fig. 3 – Cyclic loading conditions (1st & 2nd)



 

## 2. Numerical analysis and experimental result

### 2.1 Numerical modelling

To analyze the maximum shear resistance under monotonic loading condition, Finite element models (FEM) is modelled with commercial software ABAQUS. Concrete compressive strength is 35MPa, Poisson's ratio is 0.2 and elastic modulus of concrete is 20,580 MPa. Material model of concrete is suggested for Concrete damaged plasticity (CDP) model which display general capability for modeling concrete.

Steel material is modelled using an isotropic hardening material, also Poisson's ratio is 0.3 and Young's modulus is 210GPa for structural steel and 200GPa for rebar.

The loading speed is 10 mm/s and the boundary condition is shown in Figure 3.

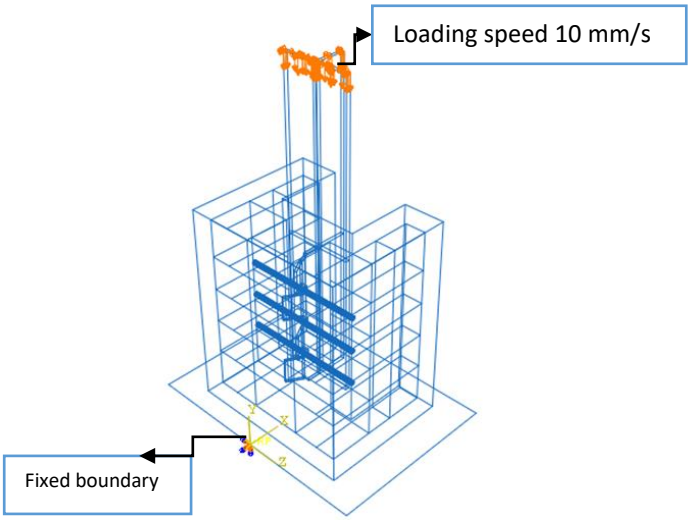


Fig. 3 – Boundary and loading condition [18]

### 2.1 Comparison between numerical analysis and experimental result

In monotonic test, the maximum shear resistance of Y4ribs-M is 468.7 kN, 776.2 kN for Y 6ribs-M. The maximum shear resistances of Y4ribs-M is 468.7 kN, 776.2 kN for Y 6ribs-M and 915.8 kN for Y 8ribs-M from numerical analysis. In Figure 5, load-slip curves of monotonic loading tests and numerical analysis are compared. The error of Y4ribs-M is 0.4%, and 4.1% for Y6ribs-M.

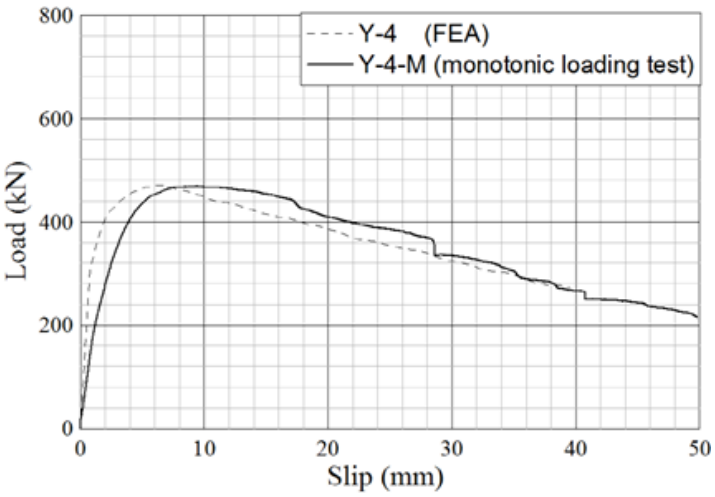


Fig. 4 – Load-slip curves from experiment and numerical analysis [18]

## 3. BWBN hysteretic model and BWBN model estimation

### 3.1 BWBN hysteretic model

Bouc-Wen model which is suggested to describe non-linear hysteretic system was first introduced by Bouc [19] and Wen [20] extended the model to produce a variety of hysteretic patterns. Later, Baber and Noori



 



[21] improved the model to include strength, stiffness and pinching degradation effects. The convenience of BWBN model is that it can be utilized for an extremely wide range of application including pinching behavior of the structure. The inelastic restoring force of a structure with hysteresis behavior is the sum of elastic and hysteric term in equation (1).

$$R(u, z)=ak_0+(1-\alpha)k_0z \quad (1)$$

Where R is the total restoring force, u is the translational displacement (elastic component), z is the hysteric displacement (hysteric component), $k_0$ is the initial stiffness and $\alpha$ is the post-yield stiffness ratio. The total restoring force (R) and hysteric displacement (z), which result from the translational displacement (u), are calculated with Newton-Rapson method [22].

Also, weight factors are applied to equation (2) to calculate an errof of the loading step. The result shows that the difference of normalized force giving the root means square error (RMSE) of the normalized force based on the hysteresis loop and the experiment data.

$$\varepsilon_F=\{½\sum_{i=1}^{N} w(F_i^{Exp}- F_i^{BWBN})^2\}^{0.5} \quad (2)$$

Where $\varepsilon_F$ is the RMSE of the normalized force, N is the number of loading steps, $F_i^{Exp}$ is the normalized force from experiment, and $F_i^{BWBN}$ is the force predicted by the BWBN model, w is the weight factor considering the amount of energy dissipation.

The following flowchart shows the preocedure to determine BWBN model with 13 parameters. Parameters $\alpha$, $\beta$, $\gamma$, k and n are shape parameters which are related to initial stiffness and the shape of the hysteresis loop. Parameter $\delta_n$ is stiffness degradation and parameter $\delta_v$ is strength degradation which are related to the deterioration in structural performance. Finally, $\xi_s$, q, p, $\psi$, $\xi_\psi$ and $\lambda$ are parameters which related to pinching behavior under cyclic loading.

### 3.2 BWBN model estimation

Through the calibration of BWBN model parameters, only parameter n is changed while the other parameters are fixed. Parameter n is sharpness of yield which is related to the maximum shear resistance.

To estimate for a certain number of ribs, the rates of increase on maximum shear resistance and parameter n from small number of ribs is used. The rate of rate of increase (ROI) of maximum shear resistance (MSR) (Y4ribs to Y6ribs) in Table 4 to ROI in parameter n (Y4ribs to Y6ribs) in Table 5 is equal to the ROI of MSR (Y4ribs to Yxribs) to ROI in n (Y4ribs to Yxribs).

Table 4 – Maximum shear resistance of each specimen by numerical analysis [18]

| Specimen | Maximum shear resistance (MSR) (kN) | Rate of increase (ROI) |
|---|---|---|
| Y4ribs | 470.9 | - |
| Y6ribs | 745.0 | 1.60 |
| Y8ribs | 915.8 | 1.94 |
| Y10ribs | 1,125.4 | 2.38 |
| Y12ribs | 1,251.4 | 2.65 |



 

Table 5 – Value estimation for parameter, n [18]

| Specimen | n | Rate of increase (ROI) |
|---|---|---|
| Y4ribs | 1.20 | - |
| Y6ribs | 2.16 | 1.80 |
| Y8ribs | 2.62 | 2.18 |
| Y10ribs | 3.21 | 2.67 |
| Y12ribs | 3.57 | 2.98 |

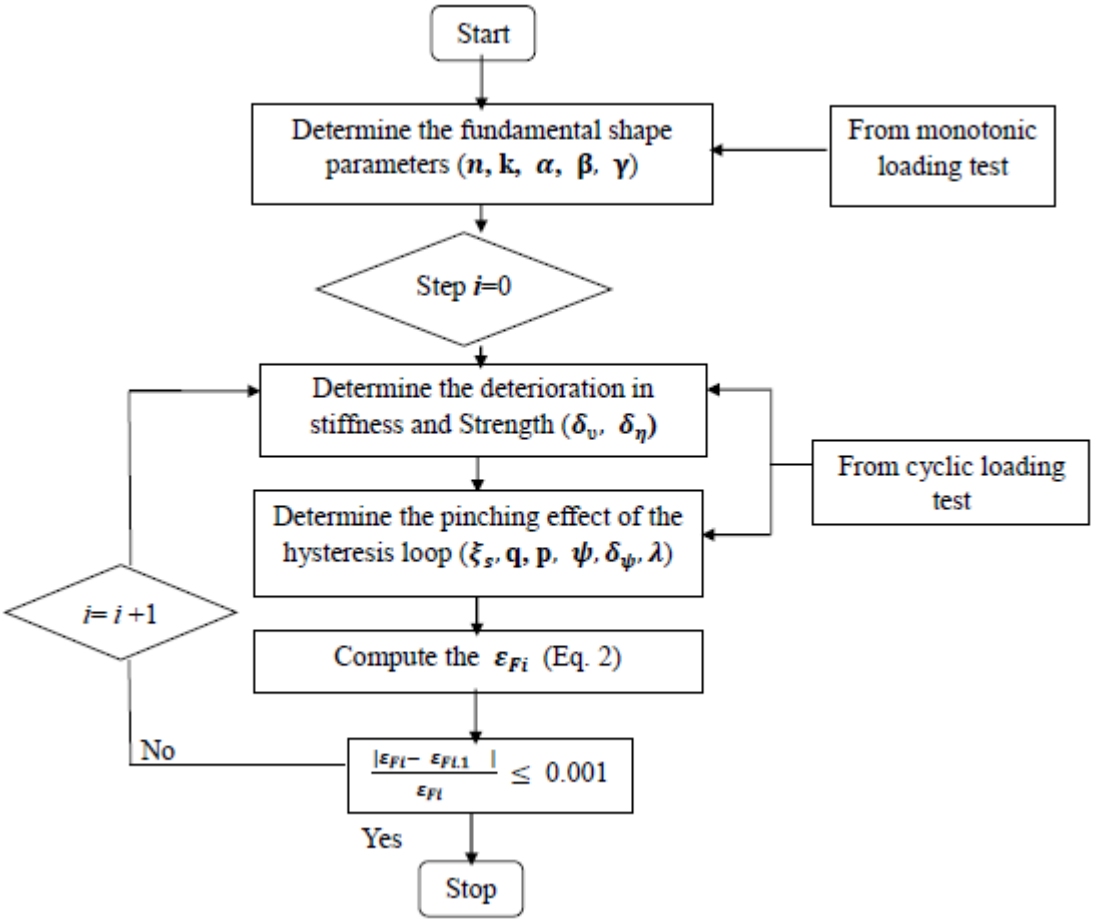


Fig. 5 – Flowchart of determination of BWBN model [18]



 

## 4. BWBN model estimation for Y-type perfobond rib shear connectors

### 4.1 BWBN model estimation in small slip (1-4 mm)

The estimation of overall slip range (1-8 mm) shows a relatively large differences due to nonlinear structural behavior under cyclic loading. To reduce the error, the slip range is divided into two part, and BWBN model is suggested for each ranges. There are relatively small slip range which is 1-4 mm slip and relatively large slip range which is 8 mm slip. Comparison between experiment results and BWBN models of Y4ribs-C, Y6ribs-C and Y8ribs-C is shown in Figure 7 to Figure 9. The error between experiment and BWBN is 1.5% for Y-4ribs-C, 0.1% for Y-6ribs-C and 8.1% for Y8ribs-C which is shown in Table 5. The BWBN parameters for small slip (1-4 mm slip range) is shown in Table 6.

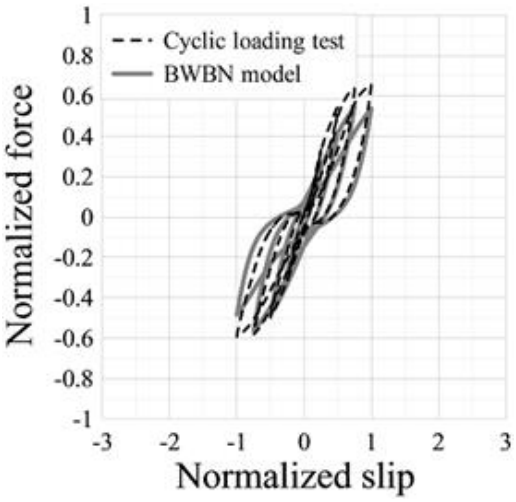


Fig. 6 – Hysteresis behavior of Y-4ribs-C (1-4 mm) [18]

Table 5 – Energy dissipation from experiment and BWBN (1-4 mm slips) [18]

| Specimen | Energy dissipation (kN mm) (1-4 mm slips) | | |
|---|---|---|---|
| | Experiment | BWBN | Difference |
| Y4ribs-C | 2,142 | 2,175 | 1.5% |
| Y6ribs-C | 2,498 | 2,501 | 0.1% |
| Y8ribs-C | 1,996 | 2,160 | 8.1% |



 

Table 6 – BWBN parameters for small slips (1-4 mm slips) [18]

| Parameter | Specimen (1-4 mm slips) | | | | |
|---|---|---|---|---|---|
| | Y 4ribs | Y 6ribs | Y 8ribs | Y 10ribs | Y 12ribs |
| α | ← | ← | -.0.015 | → | → |
| β | ← | ← | 1.500 | → | → |
| Γ | ← | ← | -0.500 | → | → |
| k | ← | ← | 1.000 | → | → |
| n | 1.160 | 2.380 | 2.930 | 3.590 | 3.990 |
| $\delta_V$ | ← | ← | 0.040 | → | → |
| $\delta_n$ | ← | ← | 0.200 | → | → |
| $\xi_s$ | ← | ← | 0.980 | → | → |
| q | ← | ← | 0.060 | → | → |
| p | ← | ← | 2.200 | → | → |
| ψ | ← | ← | 0.124 | → | → |
| $\delta_\psi$ | ← | ← | 0.010 | → | → |
| λ | ← | ← | 0.800 | → | → |
| Difference | 1.5% | 0.1% | 8.1% | | |

* ← same as right; → same as left

### 4.1 BWBN model estimation in large slip (8 mm)

Comparison between experiment results and BWBN models of Y4ribs-C, Y6ribs-C and Y8ribs-C is shown in Figure 10 to Figure 12. The error between experimental results and BWBN models is 8.4% for Y-4ribs-C, 0.1% for Y-6ribs-C and 8.9% for Y8ribs-C which is shown in Table 7. The BWBN parameters of each cases for large slip is shown in Table 8.

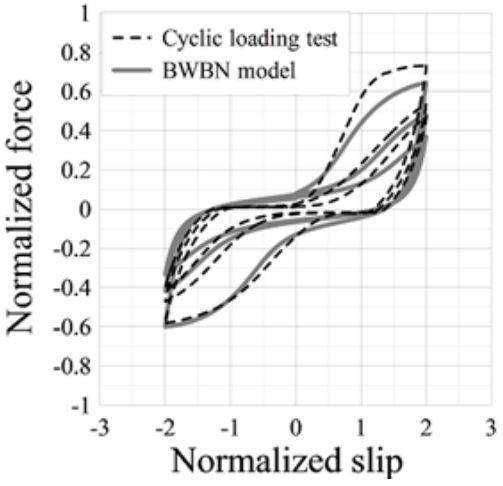


Fig. 7 – Hysteresis behavior of Y-4ribs-C (8 mm)



 

Table 7 – Energy dissipation from experiment and BWBN (8 mm slip) [18]

| Specimen | Energy dissipation (kN mm) (8mm slip) | | |
|---|---|---|---|
| | Experiment | BWBN | Difference |
| Y4ribs-C | 6,330 | 6,865 | 8.4% |
| Y6ribs-C | 10,271 | 10,280 | 0.1% |
| Y8ribs-C | 9,528 | 10,382 | 8.9% |

Table 8 – BWBN parameters for large slips (8 mm slip) [18]

| Parameter | Specimen (8 mm slips) | | | | |
|---|---|---|---|---|---|
| | Y 4ribs | Y 6ribs | Y 8ribs | Y 10ribs | Y 12ribs |
| α | ← | ← | -.0.015 | → | → |
| β | ← | ← | 1.500 | → | → |
| Γ | ← | ← | -0.500 | → | → |
| k | ← | ← | 1.000 | → | → |
| n | 1.060 | 2.180 | 2.680 | 3.350 | 3.590 |
| $\delta_V$ | ← | ← | 0.055 | → | → |
| $\delta_\Pi$ | ← | ← | 0.200 | → | → |
| $\xi_S$ | ← | ← | 0.938 | → | → |
| q | ← | ← | 0.068 | → | → |
| p | ← | ← | 1.700 | → | → |
| ψ | ← | ← | 0.100 | → | → |
| $\delta_\psi$ | ← | ← | 0.010 | → | → |
| λ | ← | ← | 0.800 | → | → |
| Difference | 8.4% | 0.1% | 8.9% | | |

* ← same as right; → same as left



 

### 4.3 Combination of small (1-4 mm) and large (8 mm) slip

The estimated hysteresis loops of each of small and large slips BWBN results are combined. As shown in Figure 13 to Figure 15, the hysteresis slip and energy dissipation of Y4ribs-C, Y6ribs-C and Y8ribs-C are represented. The error between experimental results and BWBN models is 6.7% for Y-4ribs-C, 0.1% for Y-6ribs-C and 8.3% for Y8ribs-C which is shown in Table 9.

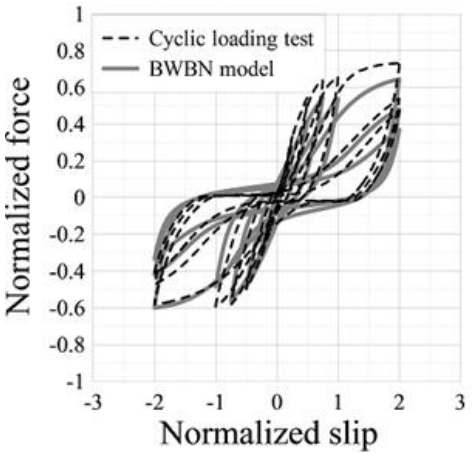


Fig. 8 – Hysteresis behavior of Y-4ribs-C (combined) [18]

Table 9 – Energy dissipation from experiment and BWBN (combined) [18]

| Specimen | Energy dissipation (kN mm) (combined) | | |
|---|---|---|---|
| | Experiment | BWBN | Difference |
| Y4ribs-C | 8,472 | 9,041 | 6.7% |
| Y6ribs-C | 12,769 | 12,782 | 0.1% |
| Y8ribs-C | 11,524 | 12,486 | 8.3% |

## 5. Conclusion

The BWBN model of stubby Y-type perfobond rib shear connector on hysteretic behaviour has been developed. In this study, the BWBN model for stubby Y-type shear connector with 8 ribs has been estimated based on the results of 4 ribs and 6ribs BWBN models. And the result of estimated BWBN model is verified with experiment result and found to be acceptable with reasonable accuracies.

Among 13 parameters which affect BWBN model, 12 parameters are fixed. The parameter n is decided from the static shear resistance of the shear connector which can be obtained from numerical FEM analysis.

The accuracy of energy dissipation can be increased by dividing small (1-4 mm) and large (8 mm) slips. Additionally, the applicability of the BWBN models on different cyclic loading condition is checked. Furthermore, conventional Y-type perfobond rib shear connector which is mainly used for bridge is planned to be manufactured to compare energy dissipating capacities between stubby and conventional Y-type perfobond rib shear connectors.

## 6. Acknowledgments

This work was supported by the Korea Institute of Energy Technology Evaluation and Planning (KETEP) and the Ministry of Trade, Industry & Energy (MOTIE) of the Republic of Korea (No. 20174030201480).



 

## 7. References

[1] Caughey, R.A., Composite Beams of Concrete and Structural Steel, In Proceedings, 41st Annual Meeting, Iowa Engineering Society (1929) (pp. 96-104).

[2] Leonhardt, F., Andrä, W., Andrä, H.P., Harre, W., New advantageous shear connection for composite structures with high fatigue strength, Beton und Stahlbetonbau, 62(12) (1987) 325-331. (in German)

[3] Ahn, J.H., Kim, S.H., Jeong, Y.J., Shear behaviour of perfobond rib shear connector under static and cyclic loadings, Mag. Concr. Res. 60 (5) (2008) 347-357.

[4] Shariati, A., Ramlisulong, N.H., Shariati, M., Various types of shear connectors in composite structures: a review, Int. J. Phys. Sci. 7 (22) (2012) 2876-2890.

[5] Oguejiofor, E.C, Hosain, M.U., A parametric study of perfobond rib shear connectors, Can. J. Civ. Eng. 21 (4) (1994) 614-625.

[6] Oguejiofor, E.C., Hosain, M.U., Numerical analysis of push-out specimens with perfobond rib connectors, Comput. Struct. 62 (4) (1997) 617-624.

[7] Kim, S.H., Lee, C.G., Ahn, J.H., Won, J.H., Experimental study on joint of spliced steel-PSC hybrid girder, part I: Proposed parallel-perfobond-rib-type joint, Eng. Struct. 33 (8) (2011) 2382-2397.

[8] Kim, S.H., Lee, C.G., Kim, S.J., Won, J.H., Experimental study on joint of spliced steel-PSC hybrid girder, part II: Full-scale test of spliced hybrid I-girder, Eng. Struct. 33 (9) (2011) 2668-2682.

[9] Kim, S.H., Ahn, J.H., Choi, K.T., Jung, C.Y., Experimental evaluation of the shear resistance of corrugated perfobond rib shear connections, Adv. Struct. Eng. 14 (2) (2011) 249-263.

[10] Machacek, J., Studnicka, J., Perforated shear connectors, Steel Compos. Struct. 2 (2002) 51-66.

[11] Kim, S.H., Choi, K.T., Park, S.J., Park, S.M., Jung, C.Y., Experimental shear resistance evaluation of Y-type perfobond rib shear connector, J. Constr. Steel Res., 82 (2013) 1-18.

[12] Kim, S.H., Park, S.J., Heo, W.H., Jung, C.Y., Shear resistance characteristic and ductility of Y-type perforbond rib shear connector, Steel Compos. Struct. 18 (2) (2015) 497-517.

[13] Kim, S.H., Heo, W.H., Woo, K.S., Jung, C.Y., Park, S.J., End-bearing resistance of Y-type perfobond rib according to rib width-height ratio, J. Constr. Steel Res. 103 (2014) 101-116.

[14] Kim, S.H., Han, O., Kim, K.S., Park, J.S., Experimental behavior of double-row Y-type perfobond rib shear connectors, J. Constr. Steel Res. 150 (2018) 221-229.

[15] Kim, S.H., Kim, K.S., Lee, D.H., Park, J.S., Han, O., Analysis of the shear behavior of stubby Y-type perfobond rib shear connectors for a composite frame structure, Materials, 10(11) (2017).

[16] Kim, S.H., Kim, K.S., Park, S., Jung, C.Y., Choi, J.G., Comparison of hysteretic performance of stubby Y-type perfobond rib and stud shear connectors, Eng. Struct. 147 (2017) 114-124.

[17] Korean Ministry of Construction and Transportation (2010). K.H.B. Specifications

[18] Kim, D. Y., Gombosuren, M., Han, O. & Kim, S. Y. (2019). Hysteretic model of Y-type perfobond rib connectors with large number of ribs.

[19] Bouc, R. (1967). Forced vibration of mechanical systems with hysteresis, Proceedings of the fourth conference on nonlinear oscillation, 315.

[20] Wen, Y. K. (1976). Method for random vibration of hysteretic systems. Journal of Engineering Mechanics, 102(2), 249-263.

[21] Baber, T. T. & Noori, M. N. (1985). Random vibration of degrading, pinching systems. Journal of Engineering Mechanics, 111(8), 1010-1026.

[22] Yu, B., Ning, C. L. & Li, B. (2016). Hysteretic model for shear-critical reinforced concrete columns. Journal of Structural Engineering, 142(9), 04016056.



 